Research Journal of Chemical Sciences _____ ISSN 2231-606X
Vol. **4(12),** 86-92, December **(2014)** *Res. J. Chem. Sci.*

What Makes a Good Weld in Terms of its Structure and Chemical Composition?

Sokolsky V. E.[1]*, Roik O. S.[1], Davidenko A. O.[1], Kazimirov V. P.[1], Lisnyak V. V.[1], Galinich V. I.[2], Goncharov I. A.[2] and Tokarev V.S.[2]

[1]Chemical Department, Taras Shevchenko National University of Kyiv, 01601 Kyiv, UKRAINE
[2]The E.O. Paton Electric Welding Institute, National Academy of Sciences of Ukraine, 03680 Kyiv, UKRAINE

Available online at: www.isca.in, www.isca.me
Received 27th November 2014, revised 12th December 2014, accepted 17th Decmeber 2014

Abstract

The difference in the carbon concentration in a weld and in a base metal causes the divergence of crystal lattice parameters and generates stresses on the boundaries between the weld and the base metal. It has been shown, on the example of carbon steels, which are solid solutions with the structure of α-Fe type, that it is possible to regulate the lattice parameter of the weld. This regulation has been performed by using the admixture of Al, Mn, and Ti metals that are supplied with a powder welding wire. The formula for the zero increment of the lattice parameter with respect to that of the α-Fe lattice of the solid solution, is proposed $\Delta a = 0.01763C_{Al} + 0.01763C_{Ti} + 0.00494C_{Mn} + 0.00188C_{C} - 0.00619C_{Si} - 0.00849C_{P} = 0$.

Keywords: Weld, parent metal, structure, crystal lattice parameter, X-ray powder diffraction, carbon steels, impact strength.

Introduction

The quality of automatic welding depends on many meaning parameters and external factors such as temperature, pressure, and gas atmosphere[1, 2]. That is why, obtaining of the high-quality welds is remained an actual task up to nowadays[2,3]. To find optimum conditions of welding for the majority of welding alloys and steels, which are free of evaporated components and carbon, is sufficient to use a welding wire of the same grade as the welded steel[4] and to protect the welding zone from harmful atmospheric constituents using a neutral flux[2,4] or an inert gas[1,5]. In the case of welding of carbon steels (CS), the concentration of carbon in the welds and in the welded metal can substantially differ due to the evaporation of the carbon combustion products[4,5]. Also, the crystal lattice parameters and the crystal structure of the welded metal could be changed at the welding and these changes are dependent on the carbon content in the parent steel[5-7]. From the crystal-chemical standpoint, CS are solid solutions with the structure of α-Fe type[6,7]. Therefore, the solid solutions can undergo the same transformation as the pure α-Fe phase. Currently, few polymorphs of α-Fe are known. The α-Fe phase (*bcc* lattice with ferromagnetic spin ordering) transforms into β-Fe at 770°C (*bcc* lattice without ferromagnetic spin ordering), the latter at subsequent heating up to 920°C transforms into γ-Fe phase with close-packed *fcc* structure[8]. The mentioned γ-Fe phase can transform into β-Fe phase at 1400°C[7]. The abovementioned polymorphs of Fe can form the solid solutions when react with various admixtures, for instance with metals and carbon. Such solid solutions have similar structures and unit cell parameters as that of the mentioned Fe polymorphs. In general, the atoms of dissolved elements distort and alter the crystal lattice of main component at the formation of the solid solutions[9]. Although these alloys can be two-and more component, they are single-phase systems, their structures are similar to the structure of the pure metal, as they belong to only the one type of crystal structure with close lattice volume and have uniform grains[7,9]. In general, the carbon forms the solid solutions of the inclusion type with all known metals. In particular, the solid solutions based on α-Fe phase with *bcc* lattice are formed by iron and carbon at the carbon low concentration. The supersaturated solid solution of carbon in the tetragonal distorted α-Fe phase, so-called martensite, is the main phase of hardened steels, which is formed at the high carbon concentration[7]. According to numerous structural studies[8], the carbon atoms are located in octahedral sites, rather than in the larger tetrahedral interstices of the α-Fe crystal lattice. Insertion of the carbon atoms into the tetrahedral voids shifts all the four surrounding atoms, while occupation of the octahedral void, by the carbon atoms, will displace only the two nearest atoms and, consequently, the lattice deformation will be realized along the direction connecting the nearest atoms in the octahedron[8]. Thus, the distortion of α-Fe lattice is anisotropic, as seen from the data depicted on figure-1a, and can transform the cubic α-Fe lattice into the tetragonal one[8]. Figure-1b shows dependence of the *c/a* ratio in the tetragonal lattice against the carbon content. A further increase of the carbon content leads to the formation of solid solutions that are based on the orthorhombic lattice[10].

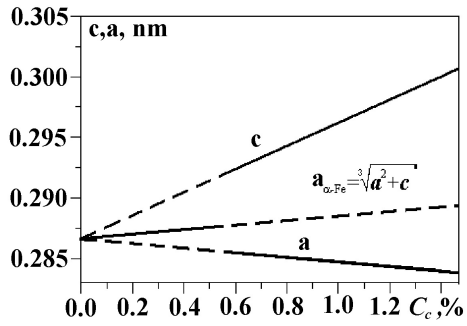

Figure-1A

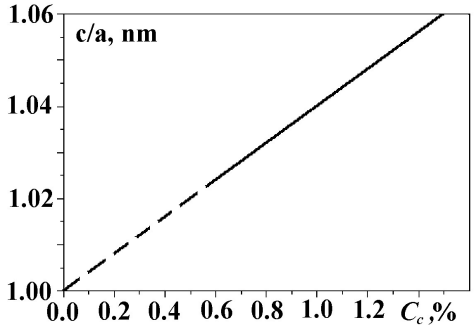

Figure-1B

Figure-1

The dependence of (a) unit cell parameters *a*, *c* and (b) the tetrahedricity degree (*c*/*a*) of the martensite lattice in the carbon steel against the concentration of carbon (C_C, at. %)

The unit cells parameters of the solid solutions, at the insignificant concentration deviations from the main composition, depend approximately linearly on the admixtures concentration[7,11]. The inclusion of impurity atoms into the lattice of the parent metal causes two effects: i. a statistically homogeneous deformation of the crystal lattice of the parent substance and ii. a local displacement, which is caused by each of the impurity atom. The values of the unit cell parameters and the interatomic distances determined from X-ray powder diffraction (XRPD) patterns are averaged over all the unit cells of the crystals. The indiscrete deformation leads to the concentration dependence of the lattice parameters of the solid solution that is registered by the XRPD method. Because of the local displacements caused by the dissolved atoms, each of the unit cells is distorted in the some degree. So, the size and the shape of the cells are varied depending on the type of substituting atom, which occupied the cell, and the occupation of neighboring cells.

The local deformation is responsible for the attenuation of X-ray reflections in the XRPD patterns. The local distortions are such that there remains a long-range order, as all the atoms are statistically deviate from some average positions. This situation corresponds to the ideal three-dimensional periodicity with the averaging period. Thus, the periodicity is a statistical, but on the average it is maintained accurately. Deviations of atoms from ideal positions should be proportional to the difference of the radii of the atoms replacing each other (Δr). The Δr parameter equals to 0.01–0.02 nm at the difference in the radii of 5–10%. The root-mean-square displacement of atoms from the averaged ideal positions ($\sqrt{\overline{u^2}}$) that can be determined from the direct X-ray diffraction experiments, gives the magnitudes of 0.01 nm in order. Apparently, the higher values of Δr and $\sqrt{\overline{u^2}}$ caused the lattice instability and the solid solution components separate to form new phases[7,9,10]. Thus, the metals with atomic radii close to iron can change the lattice parameter of solid solution of substitution-type, based on α-Fe. The lattice parameter of these solid solutions (α-Fe based) can be increased or reduced by the metals, which atomic radii are lower or higher then that of Fe, correspondingly. However, the total change of the lattice parameter should depend on the concentration of the component.

Figure-2 shows the dependence of the lattice parameter *a* against the some metals concentration in the α-Fe based solid solutions. The vertical line on the figure-2 corresponds to the limiting content of the elements in the welded stretch.

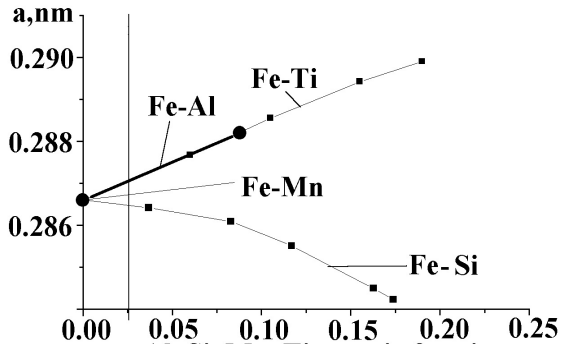

Figure-2

The dependence of *a* parameter against the content of Al, Si, Mn, and Ti in the α-Fe based solid solutions

The figure-2 shows that Al, Ti, and Mn admixtures increase the lattice parameter of α-Fe in contrast to the admixture of Si that decreases the lattice parameter[6,12]. Since, all dependences and respective curves have a linear character; consequently, they can be described for each of the components by the equations of the form:

$$y = Ax + B \quad (1)$$

As the solid solutions possess statistical character, consequently one can make assumption that the total distortion of the lattice is the sum of all the distortions introduced by each inclusion atom. The lattice parameter being under the effect only extrinsic distortion, the latter realizes if satisfied several conditions: i.

small content of dissolved components; ii. statistically uniform distribution of impurity atoms in the solvent lattice; and iii. the absence of the interaction between the impurity atoms, can be described as the sum of expressions like equation 1:

$$a = a_{Fe} + \sum_i \Delta a_i \quad (2)$$

In other words, to calculate the increase of the lattice parameter of α-Fe caused the Al, Ti, and Mn admixtures the following equation can be proposed.

$$a = 0.28663 + 0.01763C_{Al} + 0.01763C_{Ti} + 0.00494C_{Mn} - 0.00619C_{Si} \quad (3)$$

Where a is the lattice parameter accounted the impurity distortions (in nm), a_{Fe} is the lattice parameter of the solid solution based on α-Fe before the welding (in nm), Δa_i is the lattice parameter increment under the influence of *i*-impurity determined from the direct X-ray powder diffraction data taken for the samples after the welding (in nm), C_{Me} (Me = Al, Mn and Si) is the concentration of the impurity metal (in the at. %).

It should be noticed that the residual carbon, which is not taken into account in the equation 3, is presented in the weld. According to the literature[8], there is no unambiguous information about the concentration dependence of the solid solutions lattice parameters at the low concentrations of carbon in the Fe–C system[13,14], so in the figure-1, this region is shown by the dashed line for the dependences of *a* and *c*. Therefore, the lattice parameter was calculated from the assumption that tetragonal distortion is so insignificant at the low concentrations of carbon, and, in general, the isotropic deformation of the cubic lattice should realize. Consequently, if one takes into account an increase of *c* and a decrease of *a* parameter, as seen from the figure-1, the unit cell volume should be equal to $V = a \times a \times c$ for a certain concentration of carbon. Then, the *a* parameter can be determined, at the low carbon content in α-Fe, approximately, as $a \cong \sqrt[3]{V}$. Thus, the change of *a* parameter, which is caused by the contribution of carbon, can be described by the linear dependence of the form:

$$\Delta a = 0.00188C_C \quad (4)$$

The latter is appropriate and adequately describes at the low carbon concentration. This dependence is shown by the middle line on figure-1a. The region of existence of the α-$Fe_{1-x}C_x$ solid solution[13] is drawn on the figure-1b. As could be seen from the figure-1b, the lattice parameters increase significantly with an increase of the carbon content in this region. The proposed approach is valid at the low carbon concentration, when the carbon atoms are statistically distributed throughout the *bcc* cell. In general, the quantity of carbon atoms in the cell is not sufficient for direct transformation of the tetragonal lattice.

Phosphorus and sulfur are both harmful impurities that were presented in the structural steels in addition to the metallic impurities and carbon. Although the detail examination of the phase diagrams of binary Fe–P[15, 16] and Fe–S[17] systems is done, the effect of phosphorus and sulfur impurities is still beyond first-principle thermodynamic calculations. The phosphorus impurities affect the α-Fe lattice parameter and the lattice parameter dependence on the phosphorus content (C_P) can be extrapolated by the expression of the following type:

$$a = 0.28663 - 0.00849C_P \quad (5)$$

Which is correct at the low concentration of phosphorus[10,16]. The α-$Fe_{1-x}S_x$ solid solution exists for a very narrow range of x, namely, $0 < x \leq 0.00035\%$ at. of sulfur[16]. So, some authors[18] suppose that the sulfur does not dissolve in α-Fe. No data on the dependence of the lattice parameter from the sulfur content are available. Consequently, one can suppose that this low concentration of S in the solid solutions will change the lattice parameter within the error of the method and, therefore, the sulfur is not taken into account in the further calculations. Thus, the average value of the lattice of the weld should be equal to

$$a = 0.28663 + 0.01763C_{Al} + 0.01763C_{Ti} + 0.00494C_{Mn} + 0.00188C_C - 0.00619C_{Si} - 0.00849C_P \quad (6)$$

The equation 6 takes into account the effects of all the components that may contain the welding wire. Therefore, the main task of the developer of welding wire is a search for the optimum composition of each of these components. Two assumptions were done if one taking into the consideration the statistical distribution of impurities in the solid solution at the low concentration of impurities: i. All the properties of the solid solutions (with the same solvent and with the low concentration of dissolved substances) does not depend on the solute, if the lattice parameters of the solid solutions and parent metal are very close, ii. To get a quality weld its basic properties should be close to the properties of welded metal. These properties are mainly determined by the lattice parameters, so the parameters of the weld and the welded metal should be close maximally.

According to the first assumption, the carbon can be replaced by metal atoms with atomic radii close to that of the iron. This replacement should reduce the microstrains that arise at the weld–metal interface. These micro-strains can grow under the influence of external factors such as temperature, pressure and destruct the welded construction at the weld area. To test the mentioned assumptions, it has been investigated the effect of alloying components, which are contained in the welding wire, and the effect of the lattice parameter of the weld on the qualitative characteristics of the final product. For this purpose, the welded joints with different content of the alloying components were examined by means of the XRPD technique and were tested for the impact toughness.

Material and Methods

The welds preparation: The alloy structural steel of grade 10G2 (GOST 4543-71, contains 0.07–0.15% mass. of C, 0.17–0.37% mass. of Si, 1.2–1.6% mass. of Mn, ≤ 0.3% mass. of Ni, ≤ 0.035% mass. of S, ≤ 0.035% mass. of P, ≤ 0.3% mass. of Cr, and ≤ 0.3 % mass. of Cu) was used for submerged arc-welding and further studies of the obtained weld seam. This steel grade is analogue of BS 201 UK and AISI 1213 US steel grades. 10G2 is frequently utilized to produce fasteners and other constructional parts of pipe-lines that are operated at temperatures above –70°C under a gas pressure[19]. The submerged arc-welding of 10G2 grade plates was conducted using welding wire of native GA grade (∅ 0.8 mm) under the flux[20] of AN-67A grade and powders of Al, Ti, and Mn metals were used as doping admixtures. The rectangular plates (of ~1 × 1 × 0.2 cm) were cut-of from the region of the welds or from the welded metal. The cut sections were subjected to nondestructive XRPD and X-rays fluorescence (XRF) studies and to analytical techniques for the elemental analysis.

XRF analysis: The composition of samples was determined with XRF by means of a Philips X'Unique II (model 1480) wavelength-dispersive XRF spectrometer. The spectrometer was equipped with an Rh X-ray tube, operated at 50 kV and 40 mA.

Analysis for admixtures: The elemental analysis was performed for the dissolved constituents of the samples by using inductive coupled plasma optical emission Thermo Scientific iCAP 6500 Duo and flame atomic adsorption Perkin-Elmer AAnalyst 200 spectrometers.

XRPD analysis: The room temperature XRPD patterns were collected by means of a DRON-3M powder diffractometer (U = 30 kV, I = 30mA). The data were scanned over 2-theta (2θ) angular range of 40–156° with a step size of 0.02º(2θ) and a counting time of 1 sec. The studies were conducted using two X-ray sources (CuK_α with λ = 1.5418 Å and CrK_α with λ = 0.2291 nm) of the radiation. The wavelength of CuK_α radiation is close to the edge of the absorption of iron, so causes a strong fluorescence background in the XRPD patterns and lowering of the measurements accuracy. That is why, the CuK_α radiation is used only for the X-ray qualitative analysis. The crystallite size and the micro strains values, which are insensitive to changes in the concentration of impurities within the measurements error, were determined using Powder Cell 2.4 software package for the data evaluation and profile refinement[21, 22]. As the averaging of the lattice parameters for all α-Fe reflections, according to data of the least square regression (L.S.R.) method, does not give sufficient accuracy, so, the reflection of α-Fe were measured with CrK_α radiation[10] in the angular range of 2θ > 156°, that falls into the region of the precise measurements (2θ > 120°)[23] and enable to determined the lattice parameter with the accuracy of ±0.000015 nm.

Mechanic test: The impact toughness of weld seams was measured by the Charpy impact test, and, at the least three samples were conducted the test for at the least ten times to obtain the averaged value at the temperature of –20°C and –40°C.

Results and Discussion

Table-1 summarizes the results of chemical analysis of the weld samples, given in the weight and atomic %.

Figure-3 reveals that only the phases with α-Fe type crystal structure are presented in all the samples. The indexed reflexes of α-Fe phase are shown below the 2-theta axis of the graph. The numbers on the curves correspond to the samples numbering in the table 1. The XRPD patterns, XRF and chemical analysis data show that the abovementioned phases are solid solutions of the alloying components in α-Fe. Table 2 lists the structural parameters, namely, crystal lattice parameters, crystallite sizes and the microstrain values.

The obtained dependences of the lattice parameter on the content of certain components or their combinations indicate that, in general, their trends are in qualitative agreement with that represented on the figure-1. The complete compliance is hindered by the presence of other impurities in the samples.

Table-1
The chemical composition of the welds

Sample No	Element, wt. % / at. %							
	C	Mn	Si	Al	S	P	Ti	Fe
1	0.095/0.004	1.270/0.013	0.129/0.003	0.013/0.000	0.0280/0.0003	0.0140/0.0001	0.005/0.0001	98.446/0.9791
2	0.106/0.004	1.320/0.013	0.180/0.004	0.098/0.002	0.0250/0.0002	0.0120/0.0001	0.009/0.0002	98.251/0.9754
3	0.104/0.005	1.310/0.013	0.190/0.004	0.176/0.004	0.0250/0.0002	0.0120/0.0001	0.011/0.0002	96.696/0.9735
4	0.106/0.005	1.500/0.015	0.235/0.005	0.285/0.006	0.0260/0.0002	0.0140/0.0002	0.013/0.0001	97.821/0.9687
5	0.110/0.005	1.280/0.013	0.232/0.005	0.203/0.004	0.0250/0.0002	0.0120/0.0001	0.010/0.0001	98.128/0.9725
6	0.117/0.005	1.320/0.013	0.276/0.005	0.264/0.005	0.0240/0.0002	0.0100/0.0002	0.075/0.001	97.914/0.9690

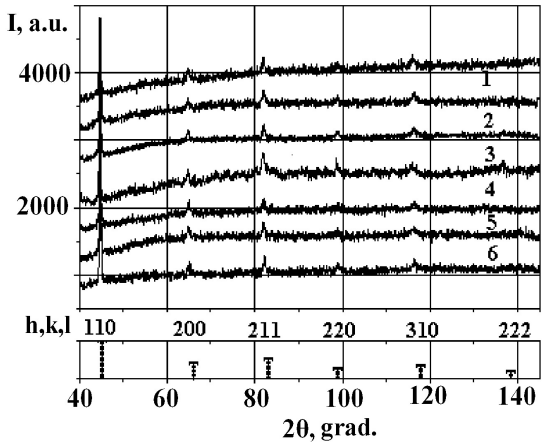

Figure-3
XRPD patterns of the welds (CuK$_\alpha$-radiation)

Table-2
Structural parameters of the samples

Sample No	Solid solution based on α-Fe lattice		
	a, nm	crystallites size, nm	Microstrain
1	0.28649	32.14	0.000523
2	0.28670	31.18	0.000787
3	0.28663	30.96	0.000529
4	0.28700	31.81	0.000666
5	0.28666	32.45	0.000689
6	0.28693	28.40	0.000683
Reference, 10G2 grade steel (α-Fe)	0.28686	41.71	0.000903

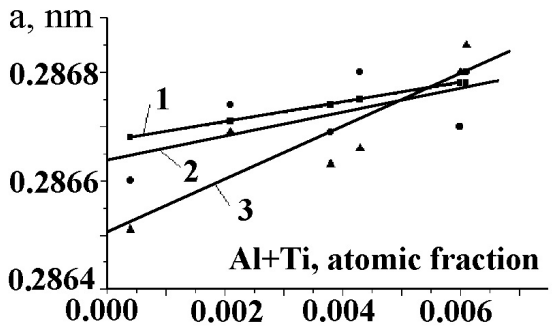

Figure-4A

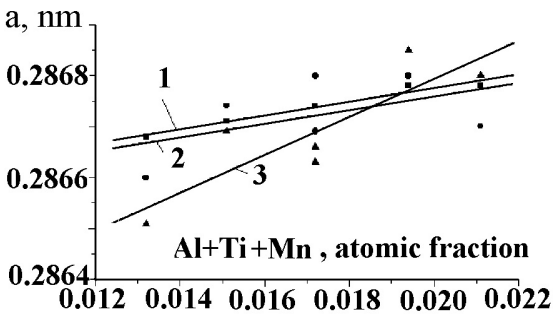

Figure-4B

Figure-4
The dependence of the lattice parameter on the content of Al + Ti (a) and Al + Ti + Mn (b) in the welds: 1 – data calculated by the equation 1; 2 – data of the precise XRD measurements; 3 – data obtained by l.s.r. method

Figure-4 shows some of these correlation dependences and imagines the observation that the value of *a* increases with an increase of (Ti + Al) and (Ti + Al + Mn) contents. Due to the influence of other impurities and a narrow concentration range of the solid solution, the overall decrease of the lattice parameter was not observed for α-Fe$_{1-x}$Si$_x$.

Figure-5a illustrates the dependences of the value of impact strength and the value of *a* against the Ti content, curves from 1 to 3 and curves from 4 to 5, respectively. Figure-5b represents the dependence of the impact strength against the value of *a*.

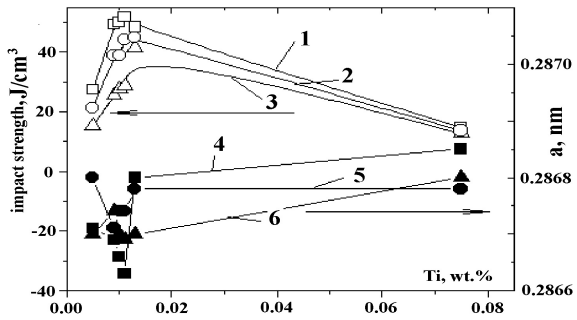

Figure-5A

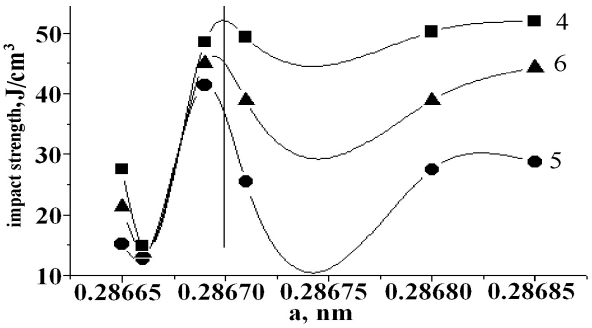

Figure-5B

Figure-5
The impact strength of welds and the lattice parameter *a* against the titanium content (a): 1 – at –20°C; 2 – the average value of the impact strength between (1) and (3); 3 – at –40°C; and the lattice parameter *a* against the titanium content (b) the impact strength of welds against the lattice parameter *a*: 4 – data calculated by the equation 4; 5 – data of the precise PXRD measurements; 6 – data obtained by l.s.r. method; a vertical line on the figure-5b corresponds to the value of the lattice parameter of the pure steel, which is beyond the welded area

The maximum value of the impact strength is found for the samples with the titanium content of 0.013% wt. So, one can suppose that the presence of the higher titanium content in the weld is not desirable. If one assumes that the increase of the lattice parameter regarding the parent steel that is used for the welding must be close to a zero, then the formula for the zero increment ($\Delta a = 0$ in the equation 2) should be as follows:

$$\Delta a = 0.01763C_{Al} + 0.01763C_{Ti} + 0.00494C_{Mn} + 0.00188C_{C} - 0.00619C_{Si} - 0.00849C_{P} = 0 \quad (7)$$

Summarizing, it should be stated that if the parameter of the crystal lattice for the parent metal and the quantity of carbon that can eliminated from CS are known, then it is possible to make a tubular flux-cored wire that contained such quantity of components (ferrosilicon and ferromanganese) that the lattice parameter of the parent metal and of the weld will coincide. The latter creates a capability to maximum improvement of the quality of welded joints.

Conclusion

It was found that if steel contains only α-Fe or the solid solution based on α-Fe and the total amount of admixtures is below 5 at. %, then the carbon constituent, which is partially com busted at arc-welding, can be replaced by the addition of the alloying components such as aluminum, titanium, manganese, and silicon. These components can be supplied by means of welding wire and/or flux to improve quality of weld by each of the alloying components and to provide a zero increase of the lattice parameter of the solid solution based on α-Fe. The content of the components that are used for such purposes should be in agreement with the proposed formula.

References

1. Sudnik W., Arc Welding, InTech, Rijeka, Croatia, 330 **(2011)**

2. Hashmi M.S.J., Comprehensive materials processing, Welding and Bonding technologies, Vol. 6, Elsevier, Amsterdam **(2014)**

3. Messler R.W., Jr. Principles of Welding, Processes, Physics, Chemistry, and Metallurgy, Wiley, N.Y., 685 **(2008)**

4. Podgaetskii V. and Kuzmenko V., Welding Slags., A Handbook, Naukova Dumka, Kiev, 253 **(1988)**

5. Deyev G.F., Surface Phenomena in Fusion Welding Processes, CRC press, Boca Raton, 424 **(2006)**

6. Smithells C.J., Metals Reference Book, Elsevier, Amsterdam, 1582 **(2013)**

7. Hume-Rothery W., Finniston H.M., Hopkins D.W. and Owen W.S., The Structures of Alloys of Iron: An Elementary Introduction, E-book, Elsevier, Amsterdam, 360 **(2013)**

8. Barrett C.S. Structure of metals. Crystallographic Methods, Principles and Data, Horney Press, Alcester, 580 **(2008)**

9. Rajagopalan M., Tschopp M.A. and Solanki K.N., Grain Boundary Segregation of Interstitial and Substitutional Impurity Atoms in Alpha-Iron, *JOM*, **66(1),** 129-138 **(2014)**

10. Gorelik S.S., Skakov Yu.A. and Rastorguev L.I. X-ray and electron-optical analysis, A textbook for high school, Third edition (in Russian), Moscow Steel and Alloys Institute, Nauka, Moscow, 360 **(2002)**

11. Vainshtein B.K., Fridkin V.M. and Indenbom V.L., Structure of Crystals, Springer, Berlin, 520 **(1994)**

12. Barabash O.M. and Koval Yu. N., Structure and properties of metals and alloys. Ser. Crystalline Structure of Metals and Alloys., Handbook, Naukova Dumka, Kiev, 600 **(1986)**

13. Okamoto H., The C-Fe (Carbon-Iron) System, *Journal of Phase Equilibria*, **13(5),** 543-565 **(1992)**

14. Franke P. and Seifert H.J., Binary System C-Fe, Landolt-Börnstein - Group IV Physical Chemistry, Ternary Steel Systems: Phase Diagrams and Phase Transition Data, Vol. 19C1, Springer, Berlin-Heidelberg, 12 **(2012)**

15. Ohtani H., Hanaya N., Hasebe M., Teraoka S. and Abe M., Thermodynamic Analysis of the Fe-Ti-P Ternary System by Incorporating First-Principles Calculations into the CALPHAD Approach, *CALPHAD*, **30,** 147-158 **(2006)**

16. Okamoto H., The Fe-P (Iron-Phosphorus) system, *Bulletin of Alloy Phase Diagrams*, **11(4),** 404 **(1990)**

17. Walder P. and Pelton A.D., Thermodynamic modeling of the Fe-S system, *Journal of Phase Equilibria and Diffusion*, **26(1),** 23-38 **(2005)**

18. Lyakishev N.P., Phase Diagrams of Binary Metal Systems*:* Handbook, V. 2, Mashinostroenie, Moscow, 1025 **(1977)**

19. Paton B.E., Biletskii S.M., Rybakov A.A., Zaitsev K.I., Mazel A.G. and Shmelev I.A., Welding of multilayer pipes in the manufacture and construction of high pressure gas pipelines, *International Journal of Pressure Vessels and Piping*, **24,** 175-187 **(1986)**

20. Sokolsky V.E., Roik O.S., Davidenko A.O., Kazimirov V.P., Lisnyak V.V., Galinich V.I. and Goncharov I.A., The phase evolution at high-temperature treatment of the oxide-fluoride ceramic flux, *Research journal of Chemical Sciences*, **4(4),** 71-77 **(2014)**

21. Kraus W. and Nolze G., Powder cell : A program for the representation and manipulation of crystal structures and calculation of the resulting X-ray powder patterns, *Journal of Applied Crystallography*, **29,** 301-303 **(1996)**

22. Kraus W. and Nolze G., Powder cell 3.2, Federal

Institute for Materials Research and Testing (BAM), available online at: http://www.ccp14.ac.uk/ccp/web-mirrors/powdcell/a_v/v_1/powder/e_cell.html, (10.01.2012), **(2012)**

23. Mirkin L.I., Handbook of X-Ray Analysis of Polycrystalline Materials, Consultants Bureau, New York, 751 **(1964)**